Title: Optimizing the Mellin-Barnes approach to numerical multiloop calculations

Author: Ievgen Dubovyk, Janusz Gluza, Tord Riemann

Citation style: Dubovyk Ievgen, Gluza Janusz, Riemann Tord. (2019). Optimizing the Mellin-Barnes approach to numerical multiloop calculations. "Acta Physica Polonica B" (Vol. 50, no. 11 (2019) s. 1993-2000), doi 10.5506/APhysPolB.50.1993

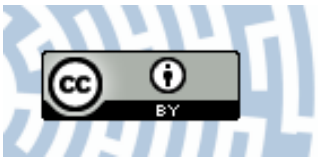

OPTIMIZING THE MELLIN–BARNES APPROACH TO NUMERICAL MULTILOOP CALCULATIONS*

Ievgen Dubovyk[a], Janusz Gluza[a,b], Tord Riemann[a]

[a]Institute of Physics, University of Silesia, Katowice, Poland
[b]Faculty of Science, University of Hradec Králové, Czech Republic

(Received November 27, 2019)

The status of numerical evaluations of Mellin–Barnes integrals is discussed, in particular the application of the quasi-Monte Carlo integration method to the efficient calculation of multidimensional integrals.

DOI:10.5506/APhysPolB.50.1993

1. Introduction

Recently, the Mellin–Barnes (MB) method [1–9] has been applied, together with the sector decomposition method [10–13], to the numerical calculation of the two-loop Feynman integrals needed in the determination of electroweak precision observables (EWPOs, for definitions and physics aspects, see *e.g.* [14]) in the Z-boson decay [15–17]. The Z resonance is formed by electron–positron collisions at the center-of-mass energy around 91 GeV. Up to 5×10^{12}, Z-boson decays are planned to be observed at projected future e^+e^- machines (ILC, CEPC, FCC-ee), when running at the Z-boson resonance [18–23]. These statistics are several orders of magnitude larger than that at LEP and would lead to very accurate experimental measurements of EWPOs — if the systematic experimental errors can be kept appropriately small too. This, in turn, means, that theoretical predictions must be also very precise, of the order of 3- to 4-loop EW and QCD effects [14].

2. Numerical integration of the Mellin–Barnes integrals: transition to the Minkowskian region

Omitting details of the construction of Mellin–Barnes representations, the final form of MB integrals suited for numerical integrations can be rep-

* Presented by I. Dubovyk at the XLIII International Conference of Theoretical Physics "Matter to the Deepest", Chorzów, Poland, September 1–6, 2019.

resented as follows:

$$I = \frac{1}{(2\pi i)^r} \int\limits_{-i\infty+z_{10}}^{+i\infty+z_{10}} \cdots \int\limits_{-i\infty+z_{r0}}^{+i\infty+z_{r0}} \prod_i^r \mathrm{d}z_i \; f_S(Z) \, \frac{\prod_j \Gamma(\Lambda_j)}{\prod_k \Gamma(\Lambda_k)} \, f_\psi(Z) \,. \qquad (1)$$

In this expression, the integration goes along paths parallel to imaginary axes and the positions of contours are fixed by z_{i0}. The Gamma functions depend on linear combinations of integration variables and some integer numbers. The function $f_S(Z)$ depends on ratios of kinematic parameters and internal masses, raised to some powers which are also linear combinations of integration variables. The part $f_\psi(Z)$ may depend on polygamma functions and constants like the Euler–Mascheroni constant γ_E; it is equal to one if the corresponding Feynman integral has no $1/\epsilon^i$ poles. We call the ratio of the gamma-type functions, $f_S(Z)$ and $f_\psi(Z)$, the core, head, and tail of the MB integral, respectively.

In order to understand the problems which appear due the transition to Minkowskian kinematics, one has to study the asymptotic behavior of integrands.

The core of MB integrals in the case of integration contours parallel to the imaginary axes, namely $z_i = z_{i0} + it_i$, is a smooth function. Its asymptotic behavior in the generalized spherical coordinates can be written as

$$\frac{\prod_j \Gamma(\Lambda_j)}{\prod_k \Gamma(\Lambda_k)} \xrightarrow[|z_i|\to\infty]{r\to\infty} \frac{\mathrm{e}^{-\beta r}}{r^\alpha} \,, \qquad \beta = \beta(\theta) \geq \pi \,, \qquad \alpha = \alpha(z_{i0}) \,. \qquad (2)$$

The asymptotic behavior of the tail $f_\psi(Z)$ can be omitted.

The head $f_S(Z)$ of the MB integral defines the most important asymptotic properties. Let us consider a typical $f_S(Z)$ which appears, for example, in MB integrals for 2-loop form-factors with one or more equal internal masses

$$\left(\frac{m^2}{-s}\right)^z = \mathrm{e}^{z \ln\left(-\frac{m^2}{s} + i\,\delta\right)} \longrightarrow \mathrm{e}^{i\,t \ln\frac{m^s}{s}} \mathrm{e}^{-\pi t} \,, \qquad s > 0 \,. \qquad (3)$$

The infinitesimal parameter δ in $s \to s + i\delta$ ($s > 0$) for the Minkowskian case comes from the causality principle and defines the correct sheet of the Riemann surface for the logarithm and the corresponding sign of the imaginary part of the integral.

As one can see, an oscillating behavior of the integrand is a natural feature of MB integrals. The main difficulties in Minkowskian kinematics come with the factor $\mathrm{e}^{-\pi t}$. For certain classes of integrals, this factor cancels the $\mathrm{e}^{-\beta r}$ part of the core along some direction or in some sector of the

integration space, and the integrand tends to 0 only as fast as $1/r^{\alpha}$. In general, such a behavior cannot easily be stabilized such that sufficiently accurate results are in reach. One should stress that the overall exponential damping factor in some cases can be restored by deforming the path of integration [24]. Alternatively, here we focus on a direct integration as a new, more general approach.

In practice, for numerical integrations, some external library like Cuba [25] is used. Usually, the integration over infinite intervals requires their transformation into finite ones; for example, in Cuba it is the interval $[0, 1]$. In the package MB.m [2], such a transformation is done in the following way:

$$t_i \to \ln\left(\frac{x_i}{1-x_i}\right), \qquad \mathrm{d}t_i \to \frac{\mathrm{d}x_i}{x_i(1-x_i)}. \tag{4}$$

This type of transformation leads to an integrable endpoint singularity and makes accurate integrations quite difficult. As an alternative, one can transform the integration interval $(-\infty, \infty)$ into $[0, 1]$ in a different way

$$t_i \to \tan\left(\pi\left(x_i - \frac{1}{2}\right)\right), \qquad \mathrm{d}t_i \to \frac{\pi \mathrm{d}x_i}{\cos^2\left(\pi\left(x_i - \frac{1}{2}\right)\right)}, \tag{5}$$

without the appearance of endpoint singularities. For more technical details see [6, 8, 9].

As an example of practical calculations, we present here results obtained for the 2-loop vertex diagram shown in Fig. 1. The MB representation for

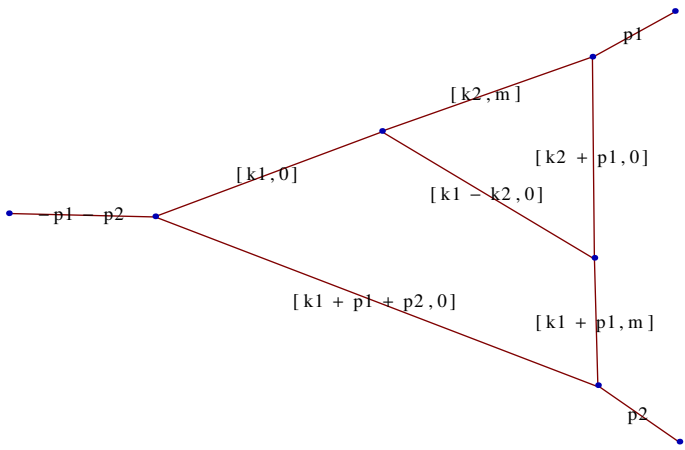

Fig. 1. An example of a 2-loop vertex diagram with $(p_1+p_2)^2 = s$ and $p_1^2 = p_2^2 = 0$. The numerical precision obtained with the MB method is discussed in the text. The diagram is drawn by the PlanarityTest.m package [26].

this diagram is three-dimensional

$$I = \frac{1}{(2\pi i)^3}\frac{1}{s^2}\int\limits_{-i\infty-\frac{47}{37}}^{i\infty-\frac{47}{37}} \mathrm{d}z_1 \int\limits_{-i\infty-\frac{44}{211}}^{i\infty-\frac{44}{211}} \mathrm{d}z_2 \int\limits_{-i\infty-\frac{176}{235}}^{i\infty-\frac{176}{235}} \mathrm{d}z_3 \left(\frac{m^2}{-s}\right)^{z_1}$$
$$\times\Gamma(-1-z_1)\Gamma(2+z_1)\Gamma(-1-z_{12})\Gamma(-z_2)\Gamma^2(1+z_{12}-z_3)\Gamma(1+z_3)$$
$$\times\Gamma(-z_3)\Gamma^2(-z_1+z_3)\Gamma(-z_{12}+z_3)/\Gamma(-z_1)\Gamma(1-z_2)\Gamma(1-z_1+z_3)\,. \quad (6)$$

The diagram has also an analytical solution [27] which makes it ideal for a non-trivial testing and comparison of different numerical techniques.

Equation (6) features a cancellation of the overall damping factor along the line $t_1 = -t_2 = t$, $t_3 = 0$. After linear transforming $z_2 \to z_2 - z_1$, the cancellation can be isolated along the t_1-axis ($t_1 = t$, $t_2 = t_3 = 0$). Numerical results for both integral versions obtained with different combinations of transformations (4) and (5) are compared with an analytical solution in Table I. In the table, the label MB1 corresponds to the numerical integration of Eq. (6), where the mapping into the integration interval $[0, 1]$ is done by the tan-type of transformation (5) for all variables. MB2 — integration of Eq. (6), tan-mapping for t_1 and t_2, ln-mapping (4) for t_3. MB3 — Eq. (6) after the transformation $z_2 \to z_2 - z_1$ and with tan-mapping for all variables. MB4 — Eq. (6) after the transformation, tan-mapping for t_1 and ln-mapping for the remaining variables. MB5 — Eq. (6), ln-mapping for all variables. All integrations are done by the Cuhre routine of the Cuba library. The maximum number of integrand evaluations allowed was set to 10^7. The

TABLE I

Numerical results for the integral Eq. (6) for $s = m^2 = 1$. AB — analytical solution [27]. MB1 to MB8 — numerical integration of the MB integrals with different integration routines and transformations of the infinite integration region as described in the text.

AB	$-1.\mathbf{199526183135}$	$+5.\mathbf{567365907880}i$	
MB1	$-1.\mathbf{199525}259137$	$+5.\mathbf{567367}419371i$	Cuhre, 10^7, 10^{-8}
MB2	$-1.\mathbf{199524}318757$	$+5.\mathbf{567365}298565i$	Cuhre, 10^7, 10^{-8}
MB3	$-1.\mathbf{199526}239547$	$+5.\mathbf{567365}843910i$	Cuhre, 10^7, 10^{-8}
MB4	$-1.\mathbf{199526183}168$	$+5.\mathbf{567365907}904i$	Cuhre, 10^7, 10^{-8}
MB5	NaN		Cuhre, 10^7
MB6	$-1.\mathbf{20}4597845834$	$+5.\mathbf{567}518701898i$	Vegas, 10^7, 10^{-3}
MB7	$-1.\mathbf{199}516455248$	$+5.\mathbf{567}376681167i$	QMC, 10^6, 10^{-5}
MB8	$-1.\mathbf{199527}580305$	$+5.\mathbf{567367}345229i$	QMC, 10^7, 10^{-6}

absolute error reported by the routine is at the level of 10^{-8}. MB6 — the same as MB5, but the integration is done by the Vegas routine [28, 29] with an error estimation of $\sim 10^{-3}$. The last two rows MB7 and MB8 show results for the numerical integration of Eq. (6) and tan-mapping for all variables with the newly presented quasi-Monte Carlo library QMC [30]. Numbers in the last column give the maximum number of integrand evaluations and the absolute error.

The instances MB4 and MB5 in Table I correspond to the integration with MB.m. They have endpoint singularities due to the ln-type of mapping for all variables. The Monte Carlo algorithm implemented in Vegas can treat such singularities, but with very low accuracy, which, in principle, correlates with the maximal number of integrand evaluations. The deterministic Cuhre algorithm is less prepared for such a singular behavior and falls to the NaN result after some number of integrand evaluations. Cases of MB1 and MB4 are already non-singular and reflect different levels of optimization of the asymptotic behavior. The most accurate result was obtained in the MB4 case. This case requires exact identification of the direction where the cancellation of the overall damping factor takes place and a rotation of integration variables such that this direction is parallel to one of the axes. In practice that can be a quite non-trivial task, especially for more-dimensional integrals or for more scales. In the case of MB1, the direction of the cancellation is not identified. The MB1 and the tan-type of mapping only fixes the endpoint singularity. One should stress that in all MB1 to MB4 cases, the error estimation is at the level of 10^{-8}, but the true number of correct digits is different all the time and does not correspond to the error (under) estimation probability returned by the program[1]. That makes Cuhre not truly reliable for such types of integrals, and it was the main motivation to develop the MBnumerics package [6, 8] which is not sensitive to this kind of problem of Cuhre. In contrast to Cuhre, the QMC library gives a stable error estimation and the requested accuracy can be obtained just by increasing the number of integration points, without any other efforts such as seeking transformation coefficients to improve the asymptotic behavior of the integrand. The obtained error is bigger than with Cuhre for the same number of integrand evaluations. This is typical for quasi-MC or Monte Carlo methods and will surpass Cuhre for more dimensional integrals.

[1] The Cuba library, together with result and absolute error, also returns a probability that the error estimate is not reliable. According to this probability, the error of 10^{-8} in the MB1 case is reliable and one would expect seven correct digits — but the number of trusted digits is only five. In the MB4 case, the error estimation is not trustable and one would expect less than seven correct digits. In practice, this is the most accurate result.

3. Conclusions

Currently, the QMC library is one of the most suitable tools for the numerical integration of MB integrals in the Minkowskian region. The library shows a linear dependence between the number of integration points and the number of correct digits in the result. This property makes it more convenient for high-dimensional integrals in contrast to deterministic or pure Monte Carlo algorithms. A combination of the appropriate transformation of the infinite integration region into a finite one with the QMC integrator allows the calculation of a wide class of MB integrals with an acceptable accuracy. All results shown here were calculated in the single-thread mode on an Intel i5 3310M mobile CPU within few minutes per case. This fact gives extra room for applications to more complicated problems and for accuracy improvements on more powerful computers. The integration of QMC into the MBnumerics package in order to get optimal accuracy and speed certainly needs further studies.

The work was supported partly by the National Science Centre, Poland (NCN) under the grant agreement 2017/25/B/ST2/01987, the international mobilities for research activities of the University of Hradec Králové, CZ.02.2.69/0.0/0.0/16 027/0008487, and the COST (European Cooperation in Science and Technology) Action CA16201 PARTICLEFACE. The participation of T.R. at MTTD2019 was kindly supported by DESY.

REFERENCES

[1] V. Smirnov, *Feynman Integral Calculus*, Springer Verlag, Berlin 2006.

[2] M. Czakon, *Comput. Phys. Commun.* **175**, 559 (2006) [arXiv:hep-ph/0511200].

[3] J. Gluza, K. Kajda, T. Riemann, *Comput. Phys. Commun.* **177**, 879 (2007) [arXiv:0704.2423 [hep-ph]].

[4] A. Smirnov, V. Smirnov, *Eur. Phys. J. C* **62**, 445 (2009) [arXiv:0901.0386 [hep-ph]].

[5] J. Gluza, K. Kajda, T. Riemann, V. Yundin, *Eur. Phys. J. C* **71**, 1516 (2011) [arXiv:1010.1667 [hep-ph]].

[6] I. Dubovyk, J. Gluza, T. Riemann, J. Usovitsch, *PoS* **LL2016**, 034 (2016) [arXiv:1607.07538 [hep-ph]].

[7] AMBRE webpage: http://prac.us.edu.pl/~gluza/ambre. Backup: https://web.archive.org/web/20180709075818/http://prac.us.edu.pl:80/~gluza/ambre/

[8] J. Usovitsch, Numerical evaluation of Mellin–Barnes integrals in Minkowskian regions and their application to two-loop bosonic electroweak contributions to the weak mixing angle of the $Z\bar{b}b$-vertex, Ph.D. Thesis, Humboldt-Universität zu Berlin, 2018, DOI:10.3204/PUBDB-2018-05160.

[9] I. Dubovyk, Mellin–Barnes representations for multiloop Feynman integrals with applications to 2-loop electroweak Z boson studies, Ph.D. Thesis, Universität Hamburg, 2019 http://ediss.sub.uni-hamburg.de/volltexte/2019/10081

[10] K. Hepp, *Commun. Math. Phys.* **2**, 301 (1966).

[11] T. Binoth, G. Heinrich, *Nucl. Phys. B* **585**, 741 (2000) [arXiv:hep-ph/0004013].

[12] A.V. Smirnov, *Comput. Phys. Commun.* **185**, 2090 (2014) [arXiv:1312.3186 [hep-ph]].

[13] S. Borowka *et al.*, *Comput. Phys. Commun.* **222**, 313 (2018) [arXiv:1703.09692 [hep-ph]].

[14] A. Blondel *et al.* (Eds.), Standard Model Theory for the FCC-ee: The Tera-Z, *CERN Yellow Reports: Monographs, Vol. 3*, (2019), DOI:10.23731/CYRM-2019-003 [arXiv:1809.01830 [hep-ph]].

[15] I. Dubovyk *et al.*, *Phys. Lett. B* **762**, 184 (2016) [arXiv:1607.08375 [hep-ph]].

[16] I. Dubovyk *et al.*, *Phys. Lett. B* **783**, 86 (2018) [arXiv:1804.10236 [hep-ph]].

[17] I. Dubovyk *et al.*, *J. High Energy Phys.* **1908**, 113 (2019) [arXiv:1906.08815 [hep-ph]].

[18] H. Baer *et al.*, The International Linear Collider Technical Design Report — Volume 2: Physics, [arXiv:1306.6352 [hep-ph]].

[19] M. Bicer *et al.*, *J. High Energy Phys.* **1401**, 164 (2014) [arXiv:1308.6176 [hep-ex]].

[20] Muhammd Ahmad *et al.*, CEPC-SPPC Study Group, CEPC-SPPC Preliminary Conceptual Design Report. 1. Physics and Detector, IHEP-CEPC-DR-2015-01, IHEP-TH-2015-01, IHEP-EP-2015-01, http://cepc.ihep.ac.cn/

[21] K. Fujii *et al.*, arXiv:1908.11299 [hep-ex].

[22] A. Abada *et al.*, *Eur. Phys. J. Spec. Top.* **228**, 261 (2019).

[23] A. Blondel *et al.*, arXiv:1901.02648 [hep-ph].

[24] A. Freitas, Y.-C. Huang, *J. High Energy Phys.* **1004**, 074 (2010) [arXiv:1001.3243 [hep-ph]].

[25] T. Hahn, *Comput. Phys. Commun.* **168**, 78 (2005) [arXiv:hep-ph/0404043].

[26] K. Bielas, I. Dubovyk, PlanarityTest 1.2.1 (August 2017), a Mathematica package for testing the planarity of Feynman diagrams, http://us.edu.pl/~gluza/ambre/planarity/, [31].

[27] U. Aglietti, R. Bonciani, *Nucl. Phys. B* **698**, 277 (2004) [arXiv:hep-ph/0401193].

[28] G.P. Lepage, *J. Comput. Phys.* **27**, 192 (1978).

[29] G.P. Lepage, Vegas: An adaptive multidimensional integration program, https://lib-extopc.kek.jp/preprints/PDF/1980/8006/8006210.pdf

[30] S. Borowka *et al.*, *Comput. Phys. Commun.* **240**, 120 (2019) [arXiv:1811.11720 [hep-ph]].

[31] K. Bielas, I. Dubovyk, J. Gluza, T. Riemann, *Acta Phys. Pol. B* **44**, 2249 (2013) [arXiv:1312.5603 [hep-ph]].